STATOR FLUX ESTIMATION FOR THREE PHASE INDUCTION MOTOR DRIVES

Augusto W. Fleury, Darizon A. de Andrade, Luciano C. Gomes
Federal University of Uberlândia, Brazil
gutofleury@gmail.com, darizon@ufu.br

***Abstract* – This paper shows and compares three different flux estimator algorithms developed for use in high-performance sensorless ac motor drives. Techniques using low pass filters, high pass filters and voltage current model are investigated. Studies are carried out for a PWM driven induction motor. The algorithms can be used to accurately measure the motor flux including magnitude and phase angle over a wide speed range. Their performances are investigated, compared, and verified using simulation. Experimental results using a fixed point DSP are also included.**

***Keywords* – Induction motor, flux estimation, pure integrator, low pass filter, high pass filter**

I. INTRODUCTION

Variable speed drive systems using induction motors continue to grow in industrial applications. With the development of new control strategies these drives have improved in efficiency and reliability. Key quantities to be known in high performance induction motor drive are the stator and/or rotor fluxes. These can be measured or estimated. Direct flux measurement requires sensors with high implementation cost and the need of modification of the machine's design. Estimating the flux is therefore visually more interesting once there is no need for physical alterations in the machine and installation costs are lower [1]-[8]. There are, in general, two methods for flux estimation: one is based on measured motor currents, and the other is based on measured voltages and currents [1]. In current model based algorithms, the motor's flux is identified by solving a set of equations in which currents, speed, or rotor position are required. Differently, the voltage model based algorithms need only the voltages and currents. The voltage model based is usually considered to be much more convenient because of its simplicity and no need of rotor position or velocity to estimate the flux, so it is more attractive for sensorless drives. In this model the flux is estimated by integrating the back electromotive force (emf) and there is only one motor parameter that needs to be known. The stator resistance in the majority of applications is measured and used with a fixed value because its variation is small with the variation of machine's speed [1].

When estimating flux from the integration of the back emf, errors in the estimation can occur. DC offsets and initial phase of the input signal to the integrator result in drift and/or offsets in the output, leading to errors in the flux estimation.

Several solutions have been presented in the literature. Some authors suggest the use of low pass filters with a very low cut off frequency to integrate the back electromotive force [1], [4]. Others suggest the use of a high pass filter to remove the dc offset of the signal before its integration. In these strategies the pure integrator can be used without drift problems [2], [8]. There are also hybrid algorithms which use current and voltage model to estimate the flux with a good accuracy over a wide speed range.

The present work shows a comparative study between three speed sensorless algorithms already presented in the literature [1],[2],[3], used to estimate the stator flux. The algorithms are described in the next section. Studies are developed for PWM driven induction motor.

II. ALGORITHMS FOR FLUX ESTIMATION

A. Algorithm with adaptive phase and magnitude compensation using low pass filter (LPF)

The expression of a pure integrator $\left(y = \frac{1}{s}x\right)$ can also be written as

$$y = \frac{1}{s+\omega_c}x + \frac{\omega_c}{s+\omega_c}z \tag{1}$$

where x is the input, z is the compensation and y is the output to the system and ω_c is the cut off frequency respectively [1].

The first term on the right hand side of (1) represents a low pass filter that is traditionally used to approximate an integrator operation. The second term can be considered as a feedback for compensating the filter output. If the output y in the second term can be appropriately adjusted and controlled, the modified function delivers a much better performance than a conventional low pass filter and the problems related to drift and initial condition normally encountered in pure integrators can be avoided.

Figure 1 shows the block diagram of the stator flux estimator that uses the concept of (1). It is based on the fact that the flux in the motor is perpendicular in time with the corresponding counter electromotive force. In this way a detector is used to verify the perpendicularity condition between the flux and the corresponding counter emf. A PI regulator is used to generate a compensation level (λ_{cmp}) sufficient to guarantee that the 90° condition is established. It is given by

$$\lambda_{cmp} = \left(k_p + \frac{k_i}{s}\right)\frac{\lambda_q \cdot emf_q + \lambda_d \cdot emf_d}{|\lambda|} \tag{2}$$

where *Kp* and *Ki* are the constants of the PI regulator.

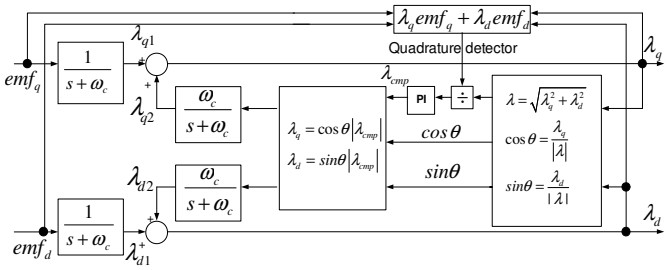

Fig. 1. Integration algorithm with adaptive compensation based in low pass filter.

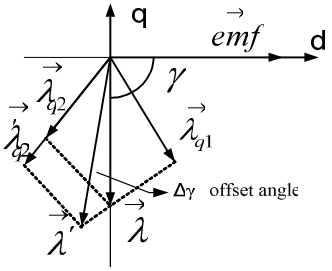

Fig. 2. Vector diagram showing relationship between $\vec{\lambda}$ and motor emf.

The operation principle of the adaptive scheme can be explained by using a vector diagram shown in Fig. 2. The estimated flux $\vec{\lambda}$ is composed of two components, a feedforward component $\vec{\lambda}_{q1}$, which is the output of the LP filter and a feedback component $\vec{\lambda}_{q2}$. In an ideal case, the flux should be orthogonal to the back emf and the output of the quadrature detector would be. When a signal with an initial value and/or dc drift is introduced into the integrator, the above orthogonality relation is lost, and the phase angle y between the flux and emf is no longer 90°, which yields an error signal defined by

$$\vec{e} = \vec{\lambda} \cdot \vec{emf} \Big/ |\lambda| = \left(\lambda_q \cdot emf_q + \lambda_d \cdot emf_d\right) \Big/ |\lambda| = |emf| \cos\gamma \tag{3}$$

When y is greater than 90° due to an increase in the feedback vector $\vec{\lambda}_{q2}$ caused by an initial value or dc drift as shown in Fig. 2, the quadrature detector will generate a negative error signal. The output of the PI regulator is reduced, and so is the feedback vector. As a result, *y* will decrease and the flux vector moves back to the original position of 90°. In this way, the adaptive scheme can keep the estimated flux and motor emf in quadrature.

This algorithm estimates the flux with a good precision in a wide speed range, with better results at higher speeds.

B. Algorithm with adaptive phase and magnitude compensation using high pass filter (HPF) and pure integrator

The block diagram of this algorithm is shown in Fig. 3 and uses a HPF to remove the DC offset normally present in the signal that will be integrated [2]. The output of the HPFs will be a sinusoidal signal but affected in magnitude and phase. Integrating the output of the first HPFs with pure integrator the response will be a sinusoidal signal with phase and magnitude distortions. To obtain an accurate flux estimative, compensations in magnitude and phase have to be performed in real time. To do so, a second level of HPFs, identical to the first level of filters, fed directly by the latter is used. Since the HPFs are identical, they will affect their input signals similarly to the first ones in terms of magnitude and phase shift. The magnitude compensation is obtained by dividing the inputs modulus by the output modulus. The coefficient for angle compensation is obtained by evaluating the difference between the input and output positions of the second group of HPFs. The effective flux position is rebuilt as shown in the following equations.

The transfer function of the HPFs is

$$HPF(s) = \frac{s}{s + \omega_c} \tag{4}$$

where

$$\omega_c = 2\pi . f_c \tag{5}$$

and f_c is the cut-off frequency.

The coefficient for gain compensation is obtained as

$$Gain = \sqrt{\frac{X_d \cdot X_d + X_q \cdot X_q}{Y_d \cdot Y_d + Y_q \cdot Y_q}} \tag{6}$$

Positions before and after the second level of HPFs are given by

$$\theta_x = \operatorname{atan2}\left(X_q, X_d\right);\ \theta_y = \operatorname{atan2}\left(Y_q, Y_d\right) \tag{7}$$

And the compensation angle is calculated as

$$Angle = \operatorname{atan2}\left(\sin\left(\theta_y - \theta_x\right), \cos\left(\theta_y - \theta_x\right)\right) \tag{8}$$

The gain compensation is applied on the signal at the output of the pure integrators for accurate flux magnitude estimation

$$\lambda_{ds0} = Gain \cdot Z_d ; \lambda_{qs0} = Gain \cdot Z_q \tag{9}$$

To obtain the corrected flux *dq0* the following equations have to be solved

$$\theta_{so} = \operatorname{atan2}\left(\lambda_{qs0}, \lambda_{ds0}\right) = \operatorname{atan2}\left(Z_q, Z_d\right) \tag{10}$$

$$\theta_s = \operatorname{atan2}\left(\sin\left(\theta_{S0} - Angle\right), \cos\left(\theta_{S0} - Angle\right)\right) \tag{11}$$

$$\lambda_{ds} = \lambda_s \cdot \cos\left(\theta_s\right);\ \lambda_{qs} = \lambda_s \cdot \sin\left(\theta_s\right) \tag{12}$$

This algorithm has a better performance in high speeds of induction motor where the errors in the flux estimation are lower.

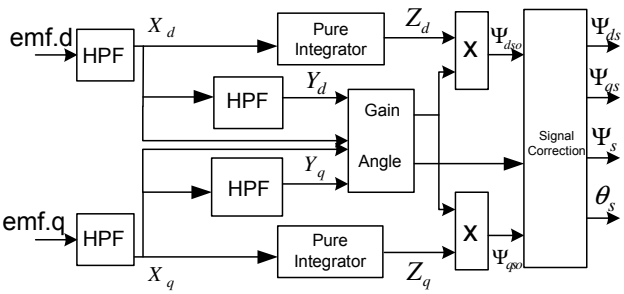

Fig. 3. Integration algorithm with adaptive compensation using high pass filter and pure integrator.

C. Flux observer algorithm using voltage and current model

This flux estimator algorithm uses the voltage and current model to estimate the estator flux with good accuracy. The open loop current model which is supposed to produce an accurate value, especially for low-speed operation, and adaptive voltage model for wide speed range operation [3]. The block diagram is shown in Fig.4.

The estimator calculates the stator flux $\vec{\lambda}_s$, the rotor flux $\vec{\lambda}_r$, the electromagnetic torque T_e, and the rotor speed ω_r solving the following equations:

$$\vec{U}_s = R_s \vec{i}_s + s\vec{\lambda}_s + j\omega\vec{\lambda}_s \quad (13)$$

$$R_r \vec{i}_r + s\vec{\lambda}_r + j(\omega - \omega_r)\vec{\lambda}_r = 0 \quad (14)$$

$$\vec{\lambda}_s = L_s \vec{i}_s + L_m \vec{i}_r \quad (15)$$

$$\vec{\lambda}_r = L_r \vec{i}_r + L_m \vec{i}_s \quad (16)$$

$$T_e = 1.5p\left(\lambda_{sd} i_{sq} - \lambda_{sq} i_{sd}\right) \quad (17)$$

where p is the number of poles and s is the derivative operator. The input parameters used in this flux estimator algorithm are the stator voltage and currents *dq,* referred to a stationary reference frame.

The rotor flux estimator in the rotor reference frame can be written as

$$\vec{\lambda}_{rdq} = \frac{L_m}{1+sT_r}\vec{i}_{sdq} - j\frac{\omega - \omega_r}{1+sT_r}\vec{\lambda}_{rdq} \quad (18)$$

where $T_r = L_r / R_r$ is the rotor time constant.

For rotor flux coordinates, the *d, q* rotor flux components in stationary reference are:

$$\lambda_{rd} = \frac{L_m}{1+sT_r} i_{sd} \;;\; \lambda_{rq} = 0 \quad (19)$$

The output of the open-loop current model is the stator flux $\vec{\lambda}_s^i$ and is written as:

$$\vec{\lambda}_s^i = \frac{L_m}{L_r}\vec{\lambda}_r^i + \frac{L_s L_r - L_m^2}{L_r}\vec{i}_s \quad (20)$$

where $\vec{\lambda}_r^i$ is the estimated rotor flux from (19).

The voltage model is based on (13) and uses the estator voltage and current measurement. For the stator reference frame the stator flux is given as

$$\vec{\lambda}_s = \frac{1}{s}\left(\vec{V}_s - R_s \vec{i}_s - \vec{U}_{comp}\right) \quad (21)$$

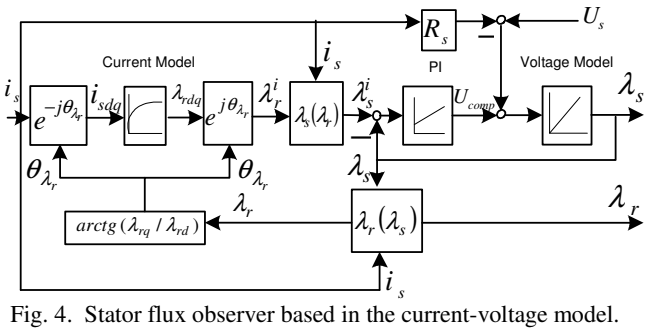

Fig. 4. Stator flux observer based in the current-voltage model.

In order to correct errors associated with pure integrator and stator resistance measurement, present in stator flux estimation, the voltage model is adapted through a PI compensator

$$\vec{U}_{comp} = \left(K_p + K_i \frac{1}{s}\right)\left(\vec{\lambda}_s - \vec{\lambda}_s^i\right) \quad (22)$$

The coefficients K_p and K_i may be calculated such that, at very low frequency, the current model stands alone, while at high frequency the voltage model prevails (23)

$$K_p = \omega_1 + \omega_2 \;;\; K_i = \omega_1 \cdot \omega_2 \quad (23)$$

where the values of the poles ω_1 and ω_2 can be configured respectively between 2-5 rad/s and 20-30 rad/s [3]. These poles have to be adjusted to have a smooth transition between the two models of the closed-loop flux estimator. A detailed parameter sensitivity analysis of this observer can be found in [9].

The rotor flux λ_r is calculated in stator reference frame by equation (24).

$$\vec{\lambda}_r = \frac{L_r}{L_m}\vec{\lambda}_s - \frac{L_s L_r - L_m^2}{L_m}\vec{i}_s \quad (24)$$

This algorithm estimates the stator flux of induction motor with a very good accuracy including practically the whole speed range.

III. SIMULATION RESULTS

Algorithms performance were verified by simulation using MATLAB/SIMULINK. The *dq* counter emfs that are the input to the estimators and the electromagnetic torque are written as:

$$emf_q = V_{qs} - R_s i_{qs} \;;\; emf_d = V_{ds} - R_s i_{ds} \quad (25)$$

$$T_e = \frac{3}{2}\cdot\frac{p}{2}\left(i_{qs}\cdot\lambda_{ds} - i_{ds}\cdot\lambda_{qs}\right) \quad (26)$$

The cut-off frequency used for the LPF of algorithm 1 was set to 6 Hz, so that the filter works in the integration region, when the motor is driven at frequencies close to rated [1].

For the algorithm 2, which uses HPF, the cut-off frequency was set to 600 Hz, which corresponds to one decade above the frequency of 60 Hz [2].

The constants K_p and K_i of the PI compensator used in algorithm 3 were set to 22 e 40 respectively [3].

The strategy followed in the simulation aiming to investigate the estimators operation was as follows: The induction motor model is solved for a given operating condition. In parallel runs the simulation of the three estimators making it possible to compare their outputs and performance with those calculated from the motor model. There are no closed loops. At the end of simulation all the outputs are available for comparison. For steady state operation at 60 Hz all the estimators worked well, with no discrepancies compared to the values calculated from the motor model.

With the motor running at steady state, initially at no load, a step of rated torque is applied during a short time interval to verify the transient behavior of the estimators. Results are reported in Figs. 5, 6 and 7, where it is seen that the response of algorithm 2 presents a bigger riple, and algorithm three with the smaller riple. It is noticed in all simulations that

algorithm three performs better that any of the other two even in low speeds. Algorithm 1 is a good choice also because it demands less computing power than algorithm 3. The worse results in all investigation were obtained from algorithm 2.

Torque estimation follows straight from flux estimation by applying eq. (26). Figure 8 shows a comparison between the torque estimated provided from all algorithms and the calculated torque from the motor model, where can be observed that all algorithms estimate the electromagnetic torque with good accuracy. Again algorithm 3 performs better than other two, particularly in speeds close to zero. This suggests that in implementation of this estimation technique can be rather useful for real time measurements of shaft torque and power delivered to the load. Conventional torque sensors are known to be rather expensive and require special installations. The instantaneous flux position is a requirement for high performance drives. Figure 9 shows the estimated flux position obtained with the studied algorithm, which as seen, compare quite well with the calculated position.

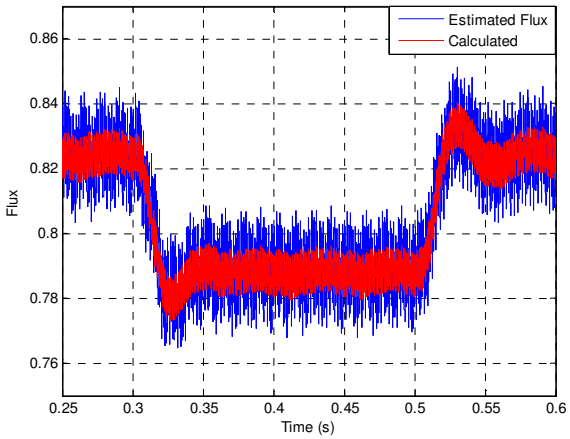

Fig. 5. Estimated and calculated stator flux amplitude (Wb) – algorithm 1 – 60 Hz.

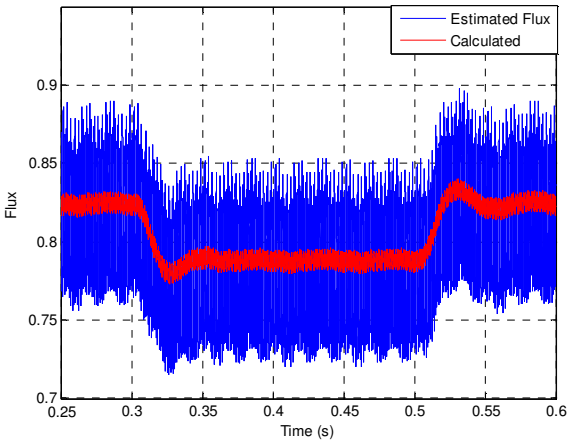

Fig. 6. Estimated and calculated stator flux amplitude (Wb) – algorithm 2 – 60 Hz.

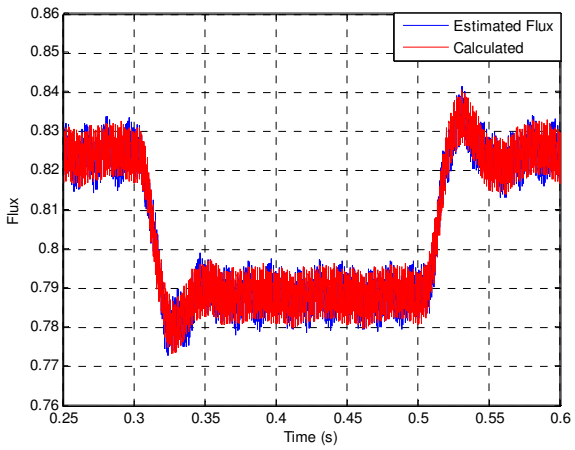

Fig. 7. Estimated and calculated stator flux amplitude (Wb) – algorithm 3 – 60 Hz.

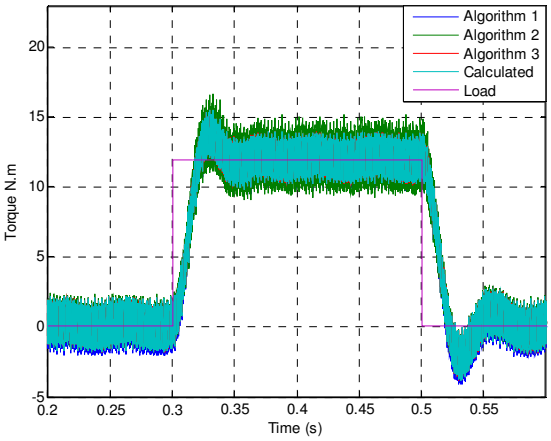

Fig. 8. Estimated and calculated torque (N.m.) – 60 Hz.

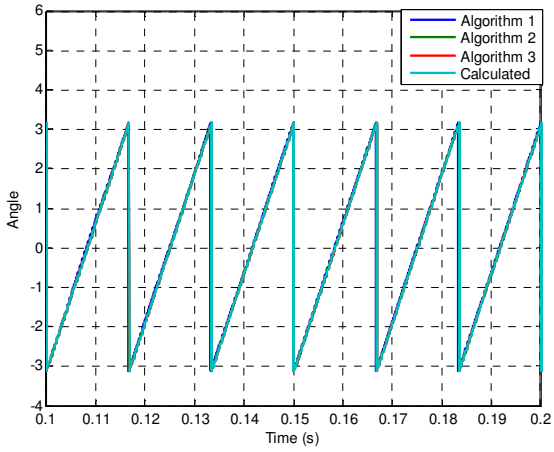

Fig. 9. Flux position – 60 Hz.

IV. EXPERIMENTAL RESULTS

The experimental setup depicted in fig. 10 was used to investigate the flux estimation algorithms and consists of a 3 HP induction machine, an IGBT inverter, a DSP kit TMS320F2812, and sensors to obtain two currents and DC link signals. With the motor connected in star configuration, only two currents were needed to be measured and the third current was calculated using (27).

$$i_c = -(i_a + i_b) \quad (27)$$

The phase voltages required for the estimation are reconstructed inside the DSP, from the DC link voltage as:

$$V_a = V_{C.C}\left(\frac{2}{3}S_1 - \frac{1}{3}S_2 - \frac{1}{3}S_3\right) \quad (28)$$

$$V_b = V_{C.C}\left(\frac{2}{3}S_2 - \frac{1}{3}S_1 - \frac{1}{3}S_3\right) \quad (29)$$

$$V_c = V_{C.C}\left(\frac{2}{3}S_3 - \frac{1}{3}S_1 - \frac{1}{3}S_2\right) \quad (30)$$

where S_1, S_2, S_3 are the switching states of PWM inverter.

Algorithms 1 and 3 were implemented and experimentally tested with the motor operating at 60 Hz, no load. Each algorithm was tested at a time. Tests were come out with the motor driven by PWM converter in open loop. Algorithm 2 was not tested.

Results obtained with algorithm 1 are reported in Fig. 11. Fig 11(a) shows the *dq* components of stator flux and Fig 11(b) shows the resultant flux amplitude. It is to be noticed that the *dq* components are in quadrature. The flux amplitude is less than rated (0.85 P.U.) because a voltage less than rated was applied. Figs 11(c) and 11(d) show respectively the flux phase angle and the phase diagram.

Results obtained with algorithm 3 are reported in Fig. 12. Fig 12(a) shows the *dq* components of stator flux and Fig 12(b) shows the resultant flux amplitude. Figs 12(c) and 12(d) show respectively the flux phase angle and the phase diagram.

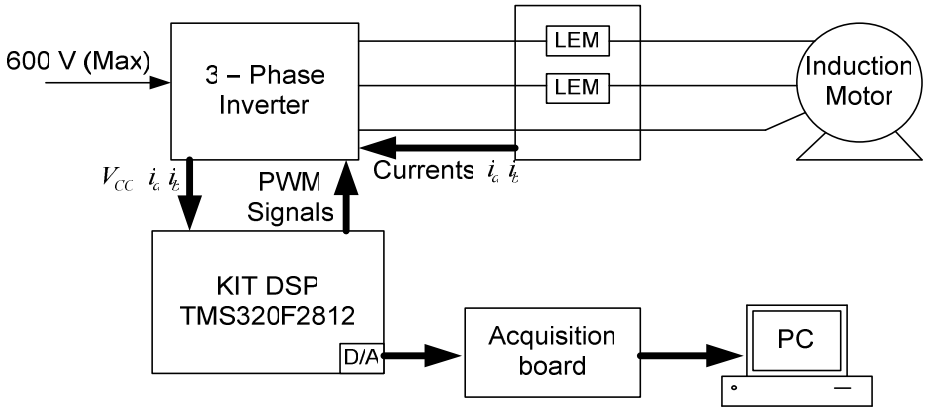

Fig.10. Experimental setup.

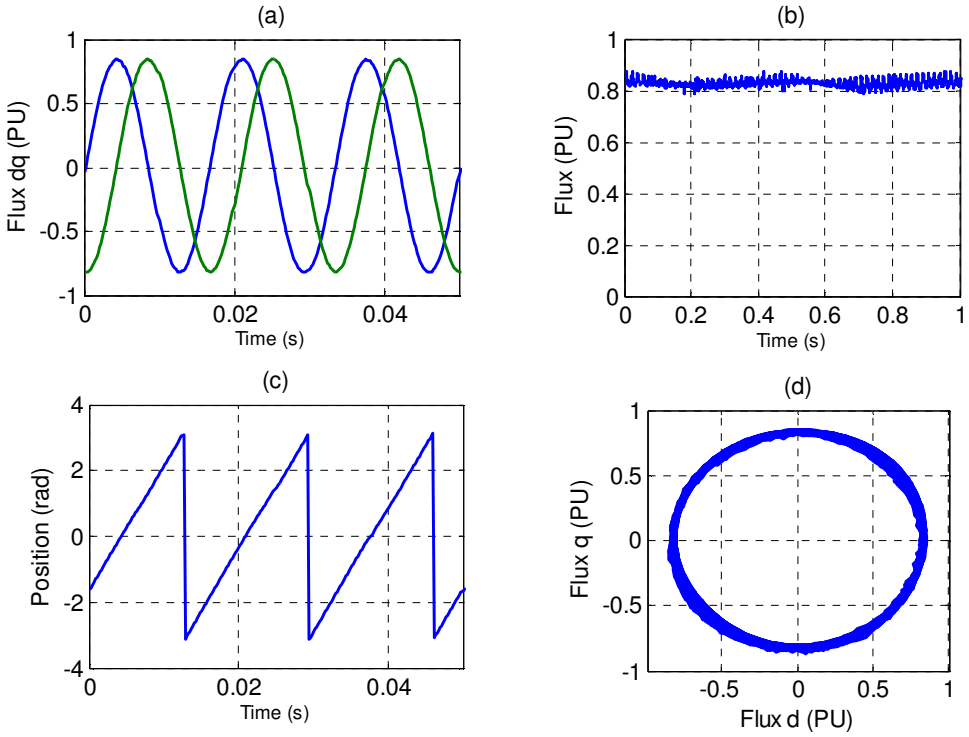

Fig. 11. Experimental results from algorithm 1

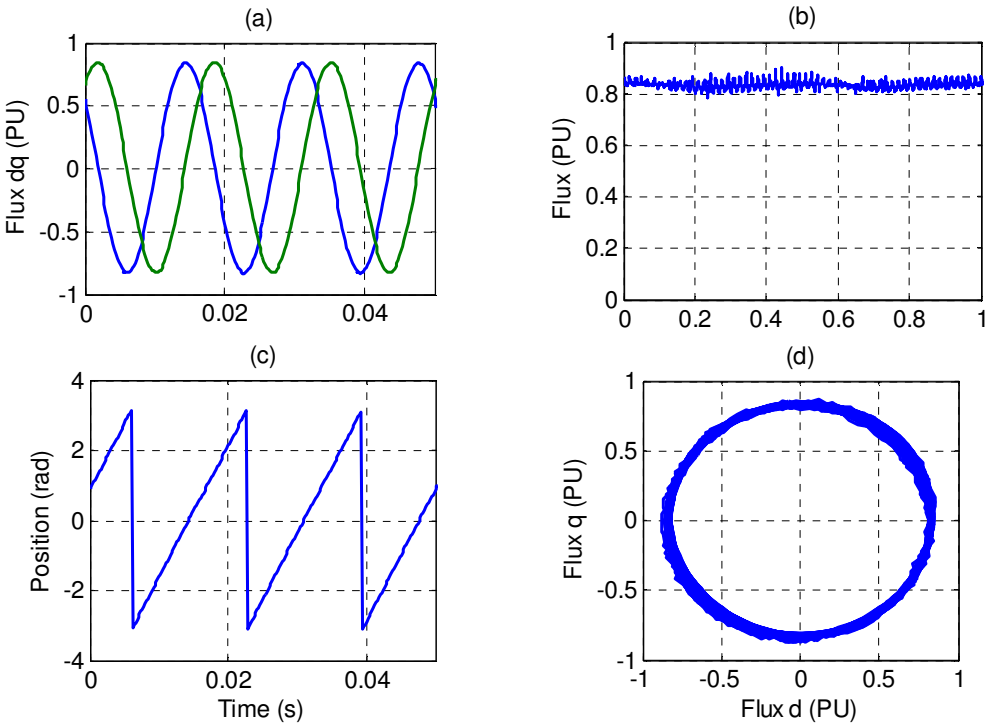

Fig. 12. Experimental results from algorithm 3

V. CONCLUSIONS

Three different flux estimators proposed in the literature were verified and implemented in digital simulations. They were tested at 60 Hz to compare performance. All of them present good estimated results in the high speed levels with supply frequencies around rated value. The algorithm that presents the best overall performance is the observer based in the voltage-current model. Experimental results using a fixed point DSP are shown and confirm the good performance of the low pass filter estimator and observer estimator.

ACKNOWLEDGMENT

Authors wish to extern their gratitude to CAPES – The Brazilian financial agency for scholarships, and Federal University of Uberlândia for offering infra structure and laboratories for the research development.

REFERENCES

[1] Hu, J.; Wu, B. New Integration Algorithms for Estimating Motor Flux over a Wide Speed Range. IEEE Trans. on P. Electronics, Vol. 13, No. 5, Setembro 1998.

[2] Zerbo, M.; Sicard, P.; Ba-Razzouk, A. Accurate Adaptive Integration Algorithms for Induction Machine Drive Over a Wide Speed Range. IEEE International Conference on Electric Machines and Drives, Page(s):1082 – 1088, Maio 2005

[3] Lascu, C.; Boldea, I.; Blaabjerg, F. A Modified Direct Torque Control for Induction Motor Sensorless Drive. IEEE Trans. on Ind. Applications, Vol. 36, No. 1, Janeiro 2000

[4] Shin, M.; Hyun, D.; Cho, S. An Improved Stator Flux Estimation for Speed Sensorless Stator flux Orientation Control of Induction Motors. IEEE Trans. on P. Electronics, Vol. 15, No. 2, Março 2000.

[5] Holtz, J.; Quan, J. Drift-and Parameter-Compensated Flux Estimator for Persistent Zero-Stator-Frequency Operation of Sensorless-Controlled Induction Motors. IEEE Trans. on Ind. Applications, Vol. 39, No. 4, Julho/Agosto 2003.

[6] Hinkkanen, M.; Luomi, J.; Modified integrator for voltage model flux estimation of induction motors. IEEE Trans. on Ind. Electronics, Vol. 50, No. 4, agosto 2003.

[7] Idris, N.; Yatim, A. An Improved Stator Flux Estimation in Steady-State Operation for Direct Torque Control of Induction Machines. IEEE Trans. on Ind. Applications, Vol. 38, No.1, Janeiro/Fevereiro. 2002.

[8] Mihalache, L. A Flux Estimator for Induction Motor Drives Based on Digital EMF Intagration With Pre- and Post- High Pass Filtering. IEEE Applied Electronics Conference and Exposition, Pg: 713-718. Vol. 2 Março 2005.

[9] Jansen,P., L.; Lorenz, R. D. A physically insightful approach to the design and accuracy assessment of flux observers for field oriented I.M.drives. IEEE Trans. on Ind. Applications, Vol. 30, pp. 101–110, Janeiro. 1994.

[10] Mitronikas, D., E.; Safacas, N., A. An Improved Sensorless Vector-Control Method for an Induction Motor Drive. IEEE Trans. on I. Electronics, Vol.52, No.6, Dezembro 2005

[11] Jansen, P. L. Observer-Based Direct Field Orientation: Analysis and Comparison of Alternative Methods. IEEE Trans. on Ind. Applications, Vol. 30, No.4, Julho/ Agosto. 1994